

BACH1 Promotes Pancreatic Cancer Metastasis by Repressing Epithelial Genes and Enhancing Epithelial-Mesenchymal Transition

Masaki Sato^{1,2}, Mitsuyo Matsumoto^{1,3}, Yuriko Saiki⁴, Mahabub Alam^{1,5}, Hironari Nishizawa¹, Masahiro Rokugo^{1,6}, Andrey Brydun¹, Shinji Yamada⁷, Mika K. Kaneko⁷, Ryo Funayama^{3,8}, Mamoru Ito⁹, Yukinari Kato^{7,10}, Keiko Nakayama^{3,8}, Michiaki Unno², and Kazuhiko Igarashi^{1,3}



ABSTRACT

Pancreatic ductal adenocarcinoma (PDAC) is among the cancers with the poorest prognoses due to its highly malignant features. BTB and CNC homology 1 (BACH1) has been implicated in RAS-driven tumor formation. We focused on the role of BACH1 in PDAC, more than 90% of which have *KRAS* mutation. Knockdown of BACH1 in PDAC cell lines reduced cell migration and invasion, in part, by increasing E-cadherin expression, whereas its overexpression showed opposite effects. BACH1 directly repressed the expression of *FOXA1* that is known to activate the expression of *CDH1* encoding E-cadherin and to inhibit epithelial-to-mesenchymal transition. BACH1 also directly repressed the expression of genes important for epithelial cell adhesion including *CLDN3* and *CLDN4*. In a

mouse orthotopic implantation model, BACH1 was required for the high metastatic ability of AsPC-1 cells. IHC analysis of clinical specimens with a newly developed anti-BACH1 mAb revealed that high expression of BACH1 is a poor prognostic factor. These results suggest that the gene regulatory network of BACH1 and downstream genes including *CDH1* contribute to the malignant features of PDAC by regulating epithelial-to-mesenchymal transition.

Significance: Greater understanding of the gene regulatory network involved in epithelial-to-mesenchymal transition of pancreatic cancer cells will provide novel therapeutic targets and diagnostic markers.

Introduction

The 5-year survival rate of individuals diagnosed with pancreatic ductal adenocarcinoma (PDAC) is 10% or less, placing PDAC among the cancers with the poorest prognoses (1). While surgical resection is currently the only treatment with a chance of a successful outcome, 80% of cases at the time of diagnosis are inoperable due to extensive metastasis. There are few effective diagnostic methods and treatments for PDAC (2). Therefore, it is an urgent matter to elucidate the

molecular mechanisms underlying the development and malignant features of PDAC. Recent genome analyses of PDAC have revealed genetic mutation profiles of PDAC (3–5). More than 90% of PDAC carry activating mutations of *KRAS* to promote their proliferation and malignant features (6).

BACH1 is a basic leucine zipper transcription factor, which represses expression of genes involved in the protection against oxidative stress such as heme oxygenase-1 (HO-1) under normal conditions. During oxidative stress, BACH1 is exported out of the nucleus, allowing for HO-1 induction and thus decrease of reactive oxygen species (7). In addition, BACH1 inhibits cellular senescence by forming a complex with p53, thereby inhibiting the expression of a subset of p53 target genes (8, 9). Therefore, BACH1 contributes to the maintenance of cell homeostasis by increasing oxidative stress and restricting tumor suppressor responses.

Recent studies have shown that BACH1 regulates the processes of cancer. BACH1 promotes methylation of CpG islands of tumor suppressor genes in cancers with *BRAF* mutation, repressing their expression (10). In breast cancer, BACH1 promotes metastasis by regulating multiple metastasis-related genes (11). It also promotes tumor formation of triple-negative breast cancer cells by repressing mitochondria-related genes (12). In a model of RAS-mediated transformation of mouse embryonic fibroblast (MEF) cells, tumor formation and proliferation are markedly inhibited in BACH1 knockout (KO) MEF as compared with wild-type (WT) MEF cells (13). These observations suggested that BACH1 might contribute to the development and malignant features of PDAC, which is often driven by activating mutation of *KRAS*. However, the function of BACH1 in PDAC is still unclear. This issue was analyzed here using siRNA-mediated gene silencing and stable overexpression in human PDAC cell lines. Direct target genes of BACH1 in PDAC cells were identified by integrating RNA-sequencing and chromatin immunoprecipitation (ChIP) and sequencing. Orthotopic implantation of CRISPR-Cas9-

¹Department of Biochemistry, Tohoku University Graduate School of Medicine, Sendai, Japan. ²Department of Surgery, Tohoku University Graduate School of Medicine, Sendai, Japan. ³Center for Regulatory Epigenome and Diseases, Tohoku University Graduate School of Medicine, Sendai, Japan. ⁴Department of Molecular Pathology, Tohoku University Graduate School of Medicine, Sendai, Japan. ⁵Department of Animal Science and Nutrition, Chattogram Veterinary and Animal Sciences University, Khulshi, Chattogram, Bangladesh. ⁶Department of Otolaryngology-Head and Neck Surgery, Tohoku University Graduate School of Medicine, Aoba-ku, Sendai, Japan. ⁷Department of Antibody Drug Development, Tohoku University Graduate School of Medicine, Sendai, Japan. ⁸Department of Cell Proliferation, Tohoku University Graduate School of Medicine, Sendai, Japan. ⁹Central Institute for Experimental Animals, Tonomachi, Kawasaki, Japan. ¹⁰New Industry Creation Hatchery Center, Tohoku University, Sendai, Miyagi, Japan.

Note: Supplementary data for this article are available at Cancer Research Online (<http://cancerres.aacrjournals.org/>).

Corresponding Authors: Kazuhiko Igarashi and Mitsuyo Matsumoto, Tohoku University Graduate School of Medicine, 2-1 Seiryō, Aoba-ku, Sendai 980-8575, Japan. Phone: 812-2717-7596; Fax: 812-2717-7598; E-mail: igarashi@med.tohoku.ac.jp; and m-matsumoto@med.tohoku.ac.jp

Cancer Res 2020;80:1279–92

doi: 10.1158/0008-5472.CAN-18-4099

©2020 American Association for Cancer Research.

Sato et al.

mediated gene knockout cells in NOG mice established that BACH1 promoted epithelial-to-mesenchymal transition (EMT) and metastasis as a key regulator of epithelial genes including *CDH1* encoding E-cadherin.

Materials and Methods

Cell culture and reagent

Human PDAC lines AsPC-1, SW1990, and BxPC-3 cells were purchased from ATCC. Human PDAC line Panc-1 was purchased from RIKEN BioResource Center. Cells were expanded within 3 passages after purchase, and multiple lots were stocked at -80°C . The *Mycoplasma* contamination check tests were performed using e-Myco plus Mycoplasma PCR Detection Kit (iNtRON). Cells were used at least less than 20 passages, but were not independently authenticated. SW1990, Panc-1, and BxPC-3 cells were cultured in RPMI1640 medium (Sigma Aldrich) supplemented with 10% FBS (Sigma Aldrich), 0.1 mg/mL penicillin/streptomycin (Gibco), and 10 mmol/L HEPES (Gibco) under humidified atmospheric conditions in 5% CO_2 . AsPC-1 was cultured similarly with 20% FBS.

siRNA, sgRNA, plasmids, and generation of stable cells

Target-specific siRNAs (Stealth RNAi siRNA Duplex Oligonucleotides, Invitrogen) were transfected using Lipofectamine RNAi-MAX (Thermo Fisher Scientific). Stealth RNAi siRNA Negative Control, Low GC (Thermo Fisher Scientific) was used as a control siRNA. To knockout *BACH1* in AsPC-1, lentiviruses were prepared by using lentiCRISPR v2 (Addgene) with single guide RNAs (sgRNA) targeting *BACH1* (see Fig. 6A). The infected AsPC-1 cells were selected by using medium supplemented with 10 $\mu\text{g}/\text{mL}$ puromycin (Sigma Aldrich). To overexpress *BACH1* in Panc-1, a vector (pCMV2-BACH1) was transfected into the cells using Fugene HD (Promega). Cells were selected in a medium with 2,000 $\mu\text{g}/\text{mL}$ G418 (Calbiochem) and cloned by isolation of surviving colonies.

Cell counting assay

Cells (300,000 cells per well) were seeded into 6-well plates, followed by transfection with 30 pmol of siRNA using Lipofectamine RNAiMAX on the next day. After the cell reseeding to dish or plate at 24 hours posttransfection, the number of live cells was measured using TC20 Automated Cell Counter (Bio-Rad Laboratories) after staining with Trypan blue.

qRT-PCR and ChIP-qPCR

Total RNA was isolated using RNeasy Plus Mini Kit (Qiagen). One microgram of total RNA was used for cDNA synthesis using Omniscript Reverse Transcription Kit (Qiagen). The ChIP-DNA was prepared using anti-BACH1 antibody (A1-6) in AsPC-1 as described (see Supplementary Methods for details). Quantitative PCR analysis was performed in LightCycler Nano (Roche) using LightCycler Fast Start DNA Master SYBR Green I (Roche). All gene expression data were normalized with an internal control gene (*ACTB*). All ChIP-qPCR data was normalized with target amplification site in Input. The primer sequences are in Supplementary Table S1.

Antibody

A new mouse mAb that specifically recognizes human BACH1 was generated with full-length human BACH1 protein expressed in SF21 cells by expression vector pFastBac (Invitrogen). BALB/c mice were

immunized by injecting the antigen with Freund's complete adjuvant. The splenocytes were fused with mouse melanoma Sp2/0 cells using polyethylene glycol method. The hybridomas were cloned by limiting dilution method and screened for antibodies against human BACH1. Anti-BACH1 mAb (clone 9D11) was purified from the culture supernatant of selected hybridoma and its specificity was validated as shown in Figs. 3A and B and 6E. Anti-BACH1 antiserum (A1-6) and anti-NRF2 antibody were reported previously (14, 15). Other antibodies were GAPDH (ab8245, Abcam), ACTB (GTX109639, GeneTeX), E-cadherin (ab1416, Abcam), p44/42 MAPK (#9102, Cell Signaling Technology), and phosphor-p44/42 MAPK (#9101, Cell Signaling Technology).

Immunofluorescent staining

The cells were fixed in 4% formaldehyde/PBS. After incubation with anti-E-cadherin (1:200) or an anti-BACH1 (1:200, 9D11) antibodies for 1 hour at 37°C , the target proteins were detected by an anti-mouse IgG FITC-conjugated secondary antibody (1:1,000, F3008, Sigma Aldrich). Nuclei were stained with 20 $\mu\text{g}/\text{mL}$ Hoechst 33342 in PBS.

Wound-healing assay

Cells in 6-well plates were grown to confluence. Monolayer of cells was scratched in a line by 1,000 μL pipette tips to remove a part of the cells. Areas of migrating cells were estimated at 24 hours later by counting numbers of pixels using ImageJ software (NIH, Bethesda, MD; <https://imagej.nih.gov/ij/>).

Transwell assay

For transwell migration and invasion assay, 24-well cell culture insert (BD Falcon, 353097) and 24-well Matrigel Invasion chamber (Corning, 354480) were used. Cells suspended in serum-free medium (AsPC-1, 200,000 cells; SW1990, 100,000 cells) were seeded to the top chamber after serum-containing medium (AsPC-1: 20% FBS; SW1990: 10% FBS) was added to bottom chamber. The cells that translocated to the bottom surface of the membrane were fixed with 4% formaldehyde and stained with 0.05% crystal violet after 24 hours and counted. The measurements were performed in technical duplicate and biological triplicate.

RNA sequencing

Libraries were constructed using Ion Total RNA-Seq Kit for AB Library Builder System (Thermo Fisher Scientific) and sequence run was performed on Ion Proton (Thermo Fischer Scientific; see Supplementary Methods for details).

ChIP sequencing

The ChIP-DNA libraries were prepared from approximately 10 ng of ChIP-DNA or Input-DNA using the Ovation Ultralow DR Multiplex System (NuGEN Technologies, 0330-32, 0331-32). The pooled libraries were sequenced as 51-base paired-end reads on an Illumina HiSeq 2500 (Illumina) across two lanes of rapid mode flow cells. Image analysis and base calling were done by Hiseq Control Software (HCS v2.2.38, Illumina) and real-time analysis software (RTA v1.18.61, Illumina). The low-quality reads marked by Illumina sequencers in the fastq format data were filtered using CASAVA v1.8. Other low-quality reads were removed by Fastx toolkit v0.0.14. The obtained reads were aligned to the hg19 human reference genome using bwa v0.7.10. The peaks were called using MACS 2 v2.1.0. The peaks existing within ± 110 bases in the different samples were judged as overlapping peaks.

High throughput data availability

The all high throughput data from this study have been deposited in Gene Expression Omnibus (<https://www.ncbi.nlm.nih.gov/geo>) under SuperSeries accession number GSE124408.

In vivo tumor growth assay and metastasis analysis

All experimental protocols in mice were approved by the Institutional Animal Care and Use Committee of Tohoku University (Sendai, Miyagi, Japan). NOD.Cg-Prkdc^{scid}Il2rg^{tm1Sug}/ShiJic (NOG) mice (6- to 8-week-old) were transplanted with 10,000 cells in 100 μ L PBS under the capsule of the pancreatic tail by laparotomy. The mice were euthanized 5 weeks after transplantation. The necropsy was performed to confirm tumor formation, liver metastasis, and peritoneal metastasis. The size of the primary tumor was measured by the pancreas weight. Liver metastasis was measured as the counted number of metastatic lesions that could be recognized visually. Peritoneal metastasis was counted as the total number of metastases of mesentery, diaphragm, and abdominal wall.

In silico analysis

RNA-sequencing data and clinical data of 176 patients with PDAC in the Cancer Genome Atlas (TCGA; <https://cancergenome.nih.gov/>) were used for Kaplan–Meier analysis.

Patients and samples for IHC

Samples were obtained from 116 cases of PDAC who underwent resection at Tohoku University Hospital (Sendai, Miyagi, Japan) from 2007 to 2014. This study was approved by the Ethics Committee of Tohoku University School of Medicine (no. 2016-1-151). All patients permitted the usage of a part of their tissue for scientific purposes and written informed consent was obtained. Tissue specimens were immediately fixated in 10% paraformaldehyde after surgery.

IHC

Paraffin sections of 3 μ m were incubated for 30 minutes at 95°C with TE (10 mmol/L Tris-HCl pH 8.0, 1 mmol/L EDTA), followed by incubation for 24 hours with primary antibodies [anti-BACH1 antibody (1:100, 9D11) or E-cadherin (1:200)]. Secondary antibody used was MAX-PO (Mouse) kit (Nichirei). Staining intensity of cancer cells was judged to be BACH1-positive, if it was more intense than that of lymphocytes used as an internal control. Staining intensity was classified into three (weak: 0%–10%, moderate: 11%–49%, strong: 50%–100%).

Results

BACH1 is important for EMT-like morphology, but not proliferation

To examine whether BACH1 regulates cell proliferation, we performed siRNA-mediated knockdown of BACH1 in AsPC-1 cells. These cells were chosen because BACH1 protein expression in AsPC-1 cells was the highest among PDAC cells examined (Supplementary Fig. S1A and S1B). When cells were seeded at high concentrations, BACH1 silencing did not affect proliferation. However, knockdown of BACH1 led to reduced cell proliferation when the initial seeding concentration was lower (Fig. 1A and B). Similar results were obtained using additional cell lines of PDAC, SW1990, and BxPC-3 cells (Fig. 1C and D; Supplementary Fig. S1C and S1D).

To investigate the influence of BACH1 on morphologic features of PDAC cells, we compared BACH1 silencing and overexpression in

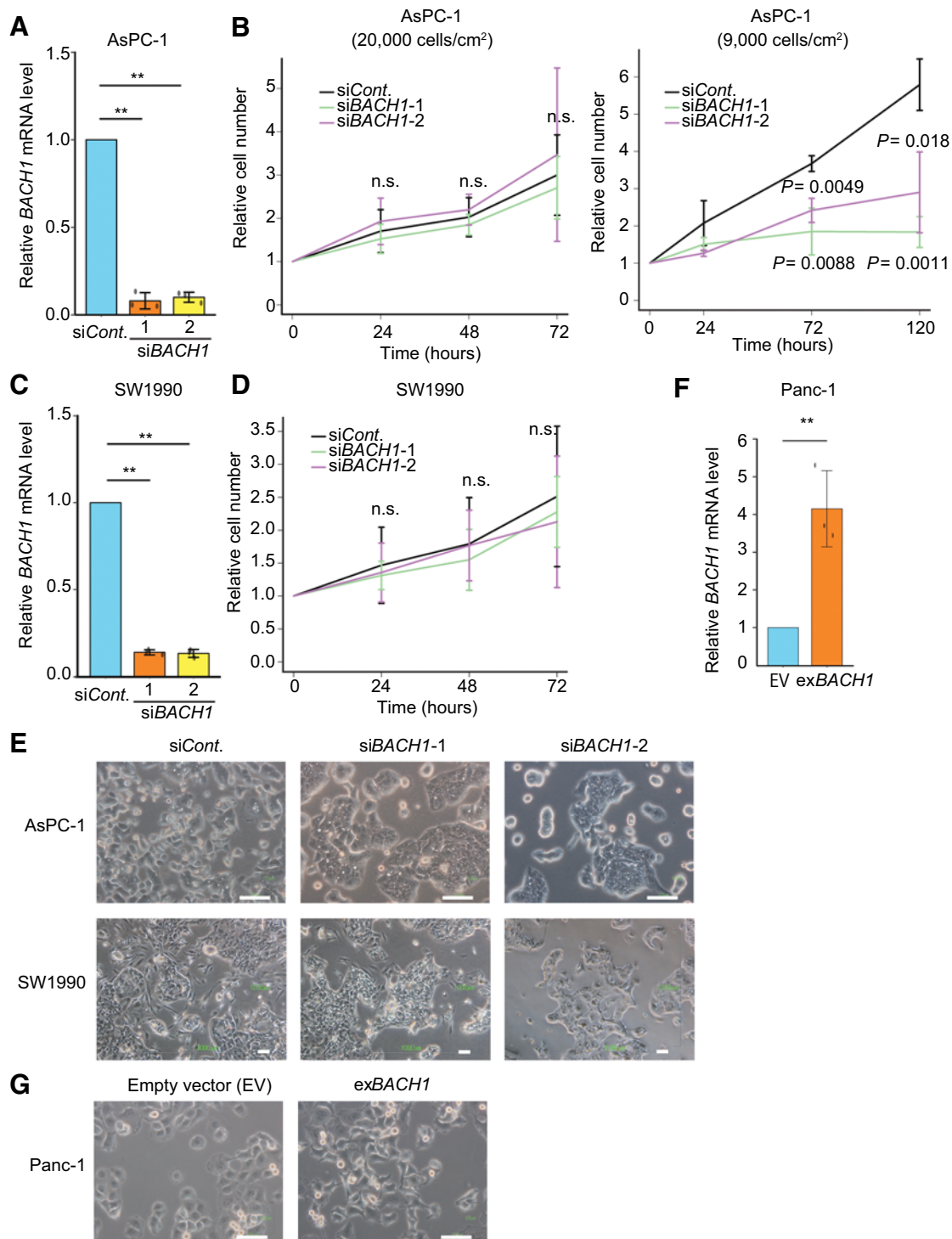
PDAC cells. BACH1 silencing apparently resulted in increased cell–cell attachment and an epithelial-like cell morphology in AsPC-1 (Fig. 1E). Such alterations were not obvious in SW1990 cells that tended to attach to each other in control conditions (Fig. 1E). To carry out gain-of-function experiments, we used Panc-1 cells that expressed relatively lower quantities of BACH1 protein among the PDAC cells examined. BACH1 overexpression in Panc-1 cells induced changes including mesenchymal-like cell morphology with decreased cell–cell adhesion (Fig. 1F and G). These observations suggested that adhesion between cells was increased, resulting in epithelial-like morphology following BACH1 silencing in AsPC-1 cells, whereas EMT-like alterations were induced by BACH1 overexpression in Panc-1 cells.

BACH1 inhibits epithelial gene expression to initiate EMT

To analyze the role of BACH1 in PDAC cells, RNA-sequencing was performed using AsPC-1 cells with or without BACH1 knockdown. Expression of 402 Ensembl gene IDs was increased, whereas 969 Ensembl gene IDs were downregulated upon BACH1 knockdown (fold change > 2, false discovery rate < 0.05; Fig. 2A; Supplementary Table S2). Because the previous experiments suggested that BACH1 might be involved in EMT (Fig. 1E and G), we focused on EMT-related genes whose expression is either reduced or induced upon EMT (16–18), and found that knockdown of BACH1 resulted in elevated expression of epithelial genes including *CDH1* encoding E-cadherin and those encoding tight junction proteins (*CLDN3*, *CLDN4*, *OCN*). Importantly, *FOXA1*, which is critical for activating the expression of epithelial genes (18, 19), was also induced upon BACH1 knockdown. In contrast, we observed decreased expression of mesenchymal genes including *VIM* encoding vimentin and *SNAI2*, a critical transcription factor necessary for EMT (Fig. 2B). These results suggest that BACH1 is critical for maintaining EMT in PDAC. To examine this possibility, we investigated transcriptional changes induced by BACH1 knockdown in AsPC-1 and SW1990 cells, and by BACH1 overexpression in Panc-1 cells using qRT-PCR (Fig. 2C). The expression of *CDH1* and *OCN*, which are epithelial-specific, was increased whereas that of *VIM*, which is mesenchymal-specific, was decreased upon knockdown of BACH1 in AsPC-1 and SW1990. Moreover, BACH1 overexpression in Panc-1 cells resulted in downregulation of *CDH1* and *OCN*, and upregulation of *VIM*. These results support the hypothesis that BACH1 is important for the maintenance of mesenchymal characteristics of PDAC cells. Importantly, *FOXA1* expression was increased by BACH1 silencing, whereas it was decreased after BACH1 overexpression (Fig. 2C). While *FOXA1* is known to be an activator of *CDH1* expression (18, 19), the double knockdown of BACH1 and *FOXA1* did not reduce *CDH1* expression (Fig. 2D), suggesting the involvement of additional transcription factors in the regulation of *CDH1* expression. *SNAI2* expression was decreased by BACH1 silencing and overexpression (Fig. 2C), suggesting a biphasic regulation of *SNAI2* by BACH1; its activation and repression being dependent on BACH1 protein levels and activity.

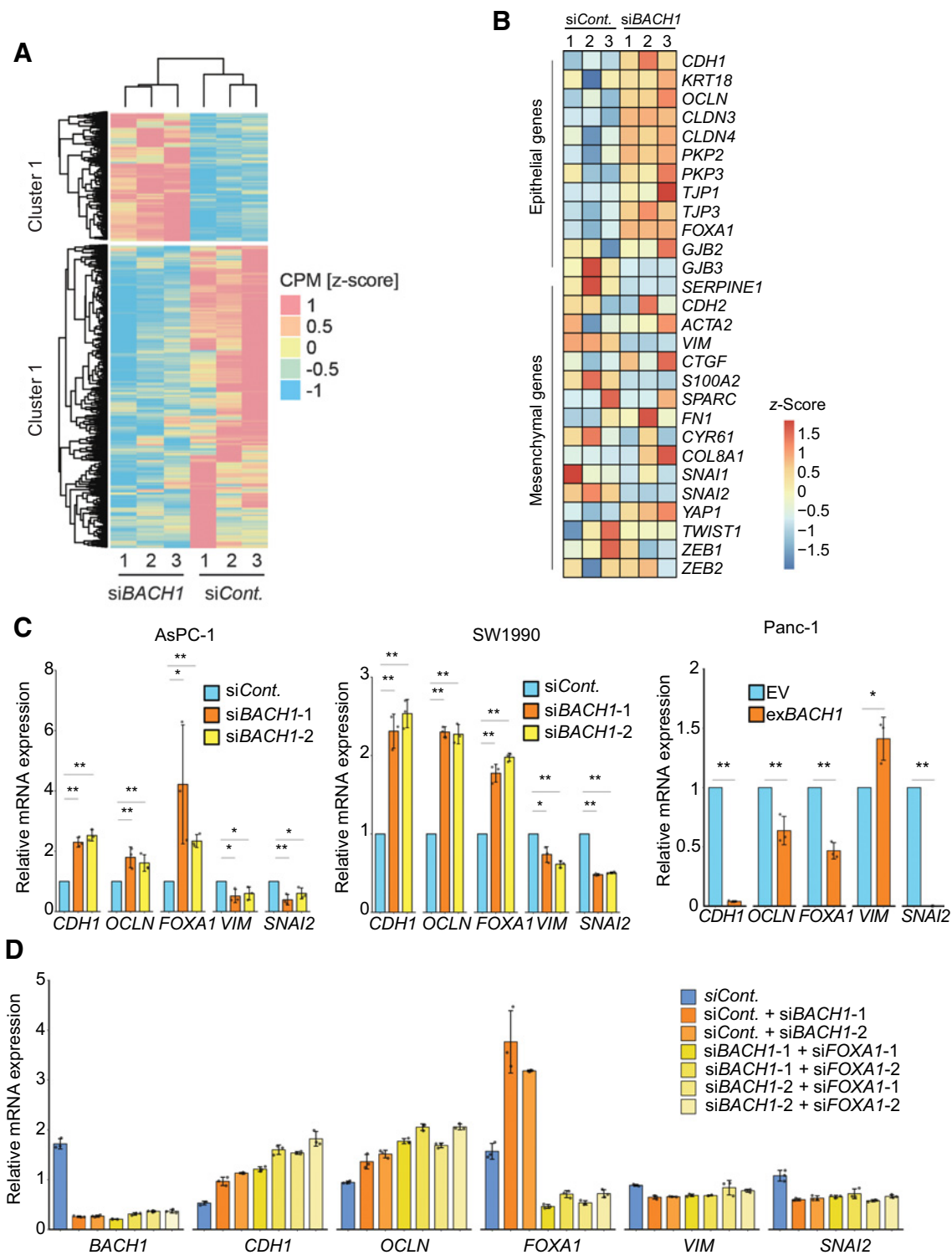
Gene ontology (GO) analysis was performed using the genes whose expression was increased or decreased by the BACH1 silencing. GO terms related to migration, wound healing, cell division, and proliferation were enriched in genes downregulated in response to BACH1 knockdown. On the other hand, in the genes whose expression was increased, we found terms related to the metabolism of anticancer drugs and cell differentiation (Supplementary Fig. S2A). KEGG pathway analysis demonstrated that the genes related to MAPK (20, 21)

Sato et al.

**Figure 1.**

BACH1 is important for mesenchymal morphologic maintenance independently of proliferation. **A**, *BACH1* mRNA levels in *BACH1*-silenced AsPC-1 cells. Scrambled siRNA was used as control. mRNA expression is normalized to the expression of control cells. **B**, Relative cell numbers of *BACH1*-silenced AsPC-1 cells; cells were seeded at 20,000 cells/cm² (left) or 9,000 cells/cm² (right) and cells were counted after 24, 48, and 72 hours. **C**, *BACH1* mRNA level in *BACH1*-silenced SW1990 cells. Scrambled siRNA was used as control. mRNA expression is normalized to the expression of control cells. **D**, Relative cell number of *BACH1*-silenced SW1990 cells. Scrambled siRNA was used as control. **E**, Morphology of *BACH1*-silenced AsPC-1 cells. Scrambled siRNA was used as control. Scale bar, 100 μ m. **F**, *BACH1* mRNA level in control and *BACH1*-overexpressing Panc-1 cells. **G**, Morphology of *BACH1*-overexpressing Panc-1 cells. Empty vector was used as control. Scale bar, 100 μ m. All data are presented as mean \pm SD, with *P* values from the Student *t* test. *, *P* < 0.05; **, *P* < 0.01; n.s., not significant.

Addition of Pancreatic Cancer to BACH1 in EMT

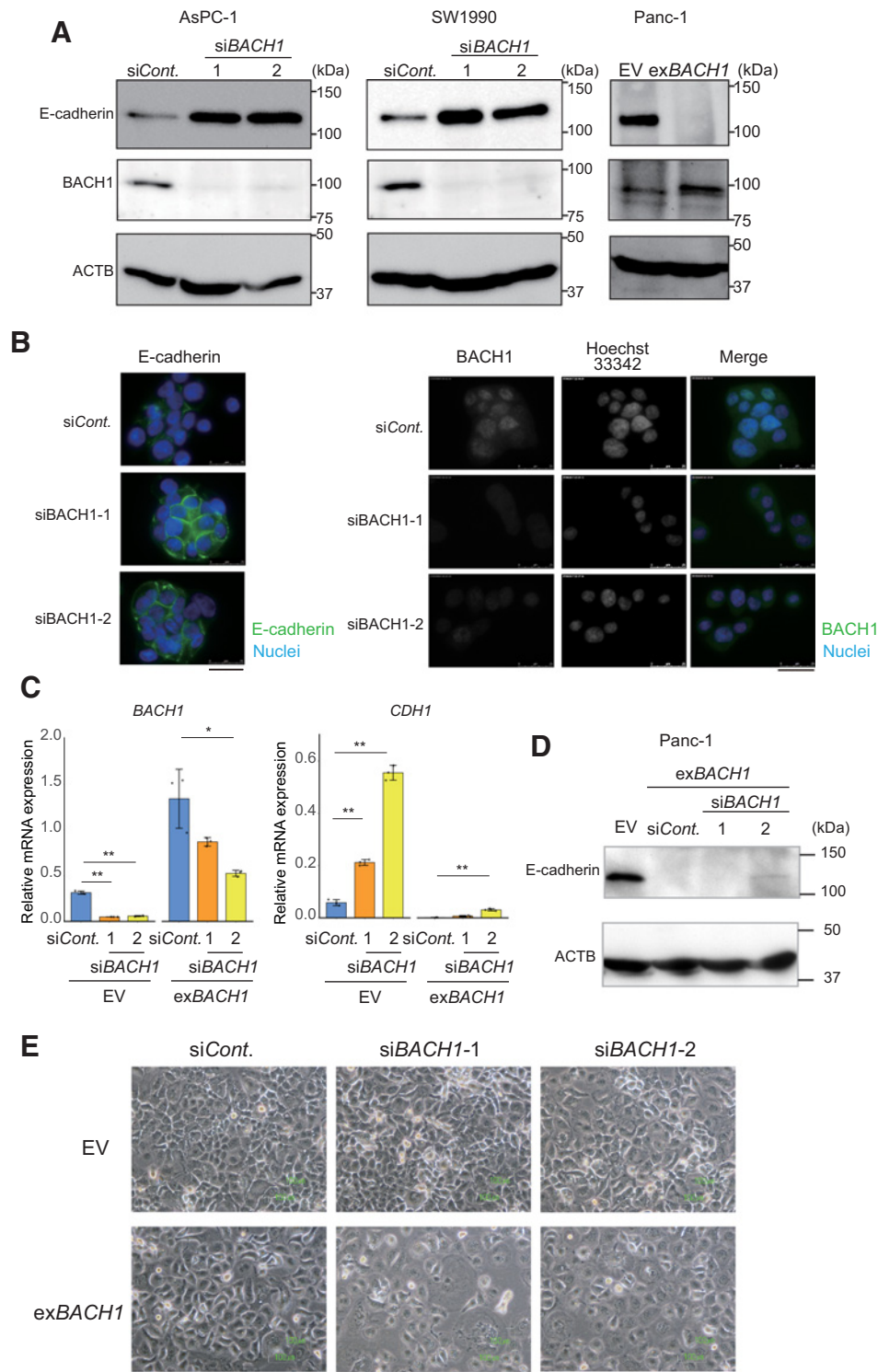
**Figure 2.**

BACH1 inhibits epithelial gene expression to initiate EMT. **A**, Heatmap of RNA sequencing results in control and *BACH1* silencing samples ($n = 3$). Scrambled siRNA was used as control. Genes with fold change ≥ 2 and $P < 0.05$ are shown. **B**, Heatmap shows the RNA sequencing results (RPKM, reads per kilobase of exon per million mapped sequence) of arbitrarily selected EMT-related genes, ignoring P value and fold change. RPKM was calculated on Cufflinks v2.2.1. **C**, qRT-PCR analyses of the indicated transcripts (relative to *ACTB*). mRNA expression is normalized to the expression of control cells. All data are presented as mean \pm SD, with P values from the Student t test. *, $P < 0.05$; **, $P < 0.01$. **D**, qRT-PCR analyses of the indicated transcripts (relative to *ACTB*) upon single or combined knockdown of *BACH1* and *FOXA1* in AsPC-1 cells. All data are presented as mean \pm SD.

Sato et al.

and TGF β pathways (22, 23), which are important for proliferation, transformation, and EMT of PDAC, were decreased in their expression upon BACH1 knockdown (Supplementary Fig. S2B). Consistent with the prediction of downregulation of MAKP, the quantity of phospho-ERK protein was reduced in BACH1 knockdown cells (Supplementary Fig. S2C). These results may explain the reduced

proliferation of AsPC-1 cells *in vitro* shown above (Fig. 1B). GSEA analysis showed also that the expression of EMT- and KRAS-related genes were altered in comparison of BACH1 knockdown cells and the control (Supplementary Fig. S2D and S2E). We surmised that activities of these pathways are suppressed by BACH1 knockdown and that BACH1 might be involved in the regulation of EMT.

**Figure 3.**

BACH1 is important for maintenance of mesenchymal characteristics. **A**, Immunoblot analysis of E-cadherin protein levels in BACH1-silenced AsPC-1 and SW1990 cells and BACH1-overexpressing Panc-1 cells. **B**, Immunofluorescence staining of E-cadherin (left) and BACH1 (right) in BACH1-silenced AsPC-1 cells. Scale bar, 25 μ m. **C**, qRT-PCR analyses of indicated transcripts (relative to ACTB as a control) in control (EV) or BACH1-overexpressing (exBACH1) Panc-1 cells with or without BACH1 knockdown. mRNA expression is normalized to the expression of the control samples. All data are presented as mean \pm SD, with *P* values from the Student *t* test. *, *P* < 0.05; **, *P* < 0.01. **D**, Immunoblot analysis of E-cadherin protein levels in control cells (EV), cells overexpressing BACH1 with (siBACH1 1 and 2) or without BACH1 knockdown (siCont.). **E**, Morphology of BACH1-overexpressing cells with or without BACH1 silencing. Empty vector and siCont. were used as controls. Scale bar, 100 μ m.

BACH1 is important for the maintenance of mesenchymal characteristics

Immunoblotting analysis indicated that the amount of E-cadherin protein was clearly increased by BACH1 silencing in AsPC-1 and SW1990 cells (Fig. 3A, left and middle). On the other hand, it was decreased by BACH1 overexpression in Panc-1 cells (Fig. 3A, right). Immunofluorescence staining of AsPC-1 cells showed that cell–cell adhesion involving E-cadherin was induced upon BACH1 knockdown (Fig. 3B, left). BACH1 protein was mainly present in the nuclei and reduced upon knockdown in AsPC-1 cells (Fig. 3B, right). Next, we examined whether the decreased E-cadherin expression in *BACH1*-overexpressing Panc-1 cells could be reversed by BACH1 knockdown. However, the reduction of BACH1 mRNA was smaller in the BACH1-overexpressing cells compared with the control cells. Nonetheless, this small reduction was associated with small inductions of E-cadherin mRNA and protein (Fig. 3C and D). Unexpectedly, BACH1-overexpressing cells showed a severely altered cell morphology with a flattened, cellular senescence-like appearance upon knockdown of BACH1 (Fig. 3E). BACH1-overexpressing Panc-1 cells seem to require continuous expression of BACH1 to maintain cellular homeostasis, the nature of which needs further investigation. These results showed that BACH1 reduces the expression of E-cadherin and formation of cell–cell adhesion, and suggests that BACH1 is important for the maintenance of mesenchymal characteristics of PDAC cells.

BACH1 promotes migration and invasion

To analyze the effect of BACH1 on cell migration, we performed wound-healing assays with AsPC-1 cells after BACH1 knockdown and with Panc-1 cells after BACH1 overexpression. Wound-healing assays using these cells demonstrated that BACH1 silencing inhibited cell migratory activity in AsPC-1 cells, whereas BACH1 overexpression in Panc-1 cells increased the activity (Fig. 4A and B). However, BACH1 silencing did not inhibit the cell migration of BxPC-3 cells, which possess WT KRAS (Supplementary Fig. S3A). BACH1 silencing did not alter the expression of EMT-related genes in BxPC-3 cells (Supplementary Fig. S3B). These results and the result of GSEA (Supplementary Fig. S2E) suggested that dependency of PDAC cells on BACH1 may be cell-type specific and dependent on the presence of mutant KRAS. To further examine whether BACH1 silencing inhibits cell migration and invasion, we carried out transwell assays using AsPC-1 and SW1990 cells. BACH1 silencing decreased cell migratory and invasive activities of these cells (Fig. 4C). Taken together, these results suggest that BACH1 is important for cell migration and invasion of PDAC cells.

BACH1 directly controls a set of EMT-related genes

To identify direct target genes of BACH1 in the induction of EMT, we performed BACH1 ChIP-seq analysis in AsPC-1 and SW1990 cells. The results of ChIP-seq were combined with the above RNA-seq results of BACH1 knockdown (Fig. 5A). Among the genes important for EMT (Fig. 2B), BACH1 directly repressed the expression of *FOXA1*, *PKP2*, *CLDN3*, and *CLDN4*, whereas it directly promoted the expression of *SNAI2* (Fig. 5B). *SNAI2* is known to repress *CDH1* expression, whereas *FOXA1* is known to induce *CDH1* expression (18, 24). *CLDN3* and *CLDN4* are molecules that constitute tight junctions and are also important for EMT suppression as like E-cadherin (17, 25, 26). *PKP2* is a constituent protein of the desmosome that is involved in cell–cell adhesion (27). ChIP-qPCR results confirmed that BACH1 bound the genomic regions of *FOXA1* and *SNAI2* in AsPC-1 and SW1990 cells

(Fig. 5C). We surmise that BACH1 regulates a set of EMT-related genes by repressing critical epithelial genes and by activating *SNAI2* to initiate EMT.

BACH1 promotes metastasis but not tumor formation

We established AsPC-1 cells lacking BACH1 using a CRISPR/Cas9 system. Knockout was performed using two different constructs of sgRNA (Fig. 6A), and the mutations were confirmed by Sanger sequencing. Expression of *CDH1*, *OCLN* and *FOXA1* was upregulated in BACH1 knockout cells. However, expression of *VIM* and *SNAI2* was not altered (Fig. 6B). We investigated E-cadherin expression by immunoblotting and immunofluorescence analyses (Fig. 6B and C; Supplementary Fig. S4A and S4B). E-cadherin expression was upregulated in sgBACH1-2, but this effect was smaller in sgBACH1-1. We observed consistent alterations in BACH1 mRNA and protein amounts in the knockout, RNA silencing, and overexpressing cells except BACH1 mRNA in knockout cells (Supplementary Fig. S4C and S4D, see below). Because amounts of NRF2 protein were similar between control and manipulated cells, alterations of oxidative stress appeared negligible upon manipulation of BACH1. Also, the differences in BACH1 mRNA and protein in AsPC-1 and Panc-1 cells were not due to differences in oxidative stress or NRF2.

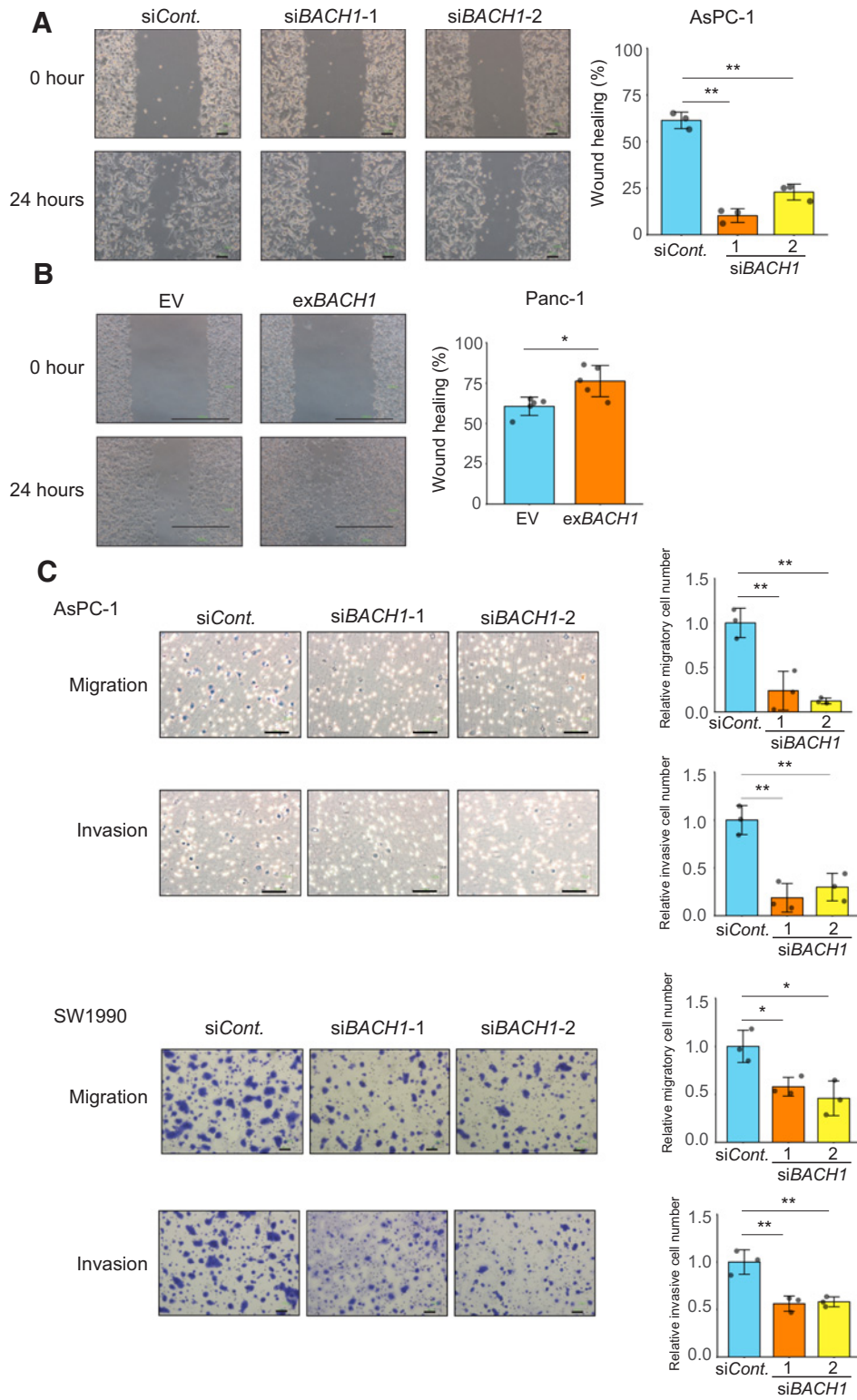
To compare gene expression in these cells further, RNA-seq was performed using control AsPC-1/sgCont cells and BACH1 knockout AsPC-1/sgBACH1-2 cells. While the amounts of BACH1 mRNA were not greatly reduced by BACH1 knockout (Supplementary Figs. S4C and S5A), the presence of the intended or unintended mutations were confirmed from RNA-seq reads (Supplementary Fig. S5B). Comparison of gene expression patterns in these cells using all genes (reads counts > 5 and CPM > 1 in more than one sample) showed that the effects of siRNA and CRISPR/Cas9 were not the same (Supplementary Fig. S5C and S5D; Supplementary Table S3), suggesting an adaptation of the cells to the BACH1 knockout. Consistent with the above results of BACH1 silencing, BACH1 knockout resulted in elevated expression of epithelial genes including *FOXA1* and *CLDN3* (Supplementary Fig. S5E–S5G; Supplementary Tables S2 and S3). Repression of these genes might be especially important for the function of BACH1 in PDAC cells. In contrast, expression of mesenchymal genes and RAS-related genes was decreased by the BACH1 knockout (Supplementary Figs. S5E and S5F and S6A and S6B). These results further support the hypothesis that BACH1 is important for the maintenance of mesenchymal characteristics and KRAS signaling of PDAC cells.

To examine whether BACH1 would be involved in tumor formation and/or metastasis, we compared the effects of BACH1 knockout on PDAC formation and metastasis in an orthotopic mouse model. After orthotopic transplantation to NOG mice, AsPC-1/sgCont cells and AsPC-1/sgBACH1-2 cells generated primary tumors in the pancreas and metastases in the liver, mesentery, diaphragm, and peritoneum that were examined five weeks later (Supplementary Fig. S6C). We compared primary tumor formation between control and BACH1 knockout AsPC-1 by measuring the weight of pancreas. We counted the number of liver metastases and peritoneal metastases (mesentery, diaphragm, and abdominal wall). Primary tumor weight was not different between the two experimental sets. In contrast, lower quantities of liver and peritoneal metastatic foci were observed in mice containing BACH1 knockout AsPC-1 cells than those containing control cells (Fig. 6D). BACH1 was strongly stained in nuclei of AsPC-1/sgCont while barely present in AsPC-1/sgBACH1-2 cells of the pancreas and liver at 5 weeks posttransplantation (Fig. 6E).

Sato et al.

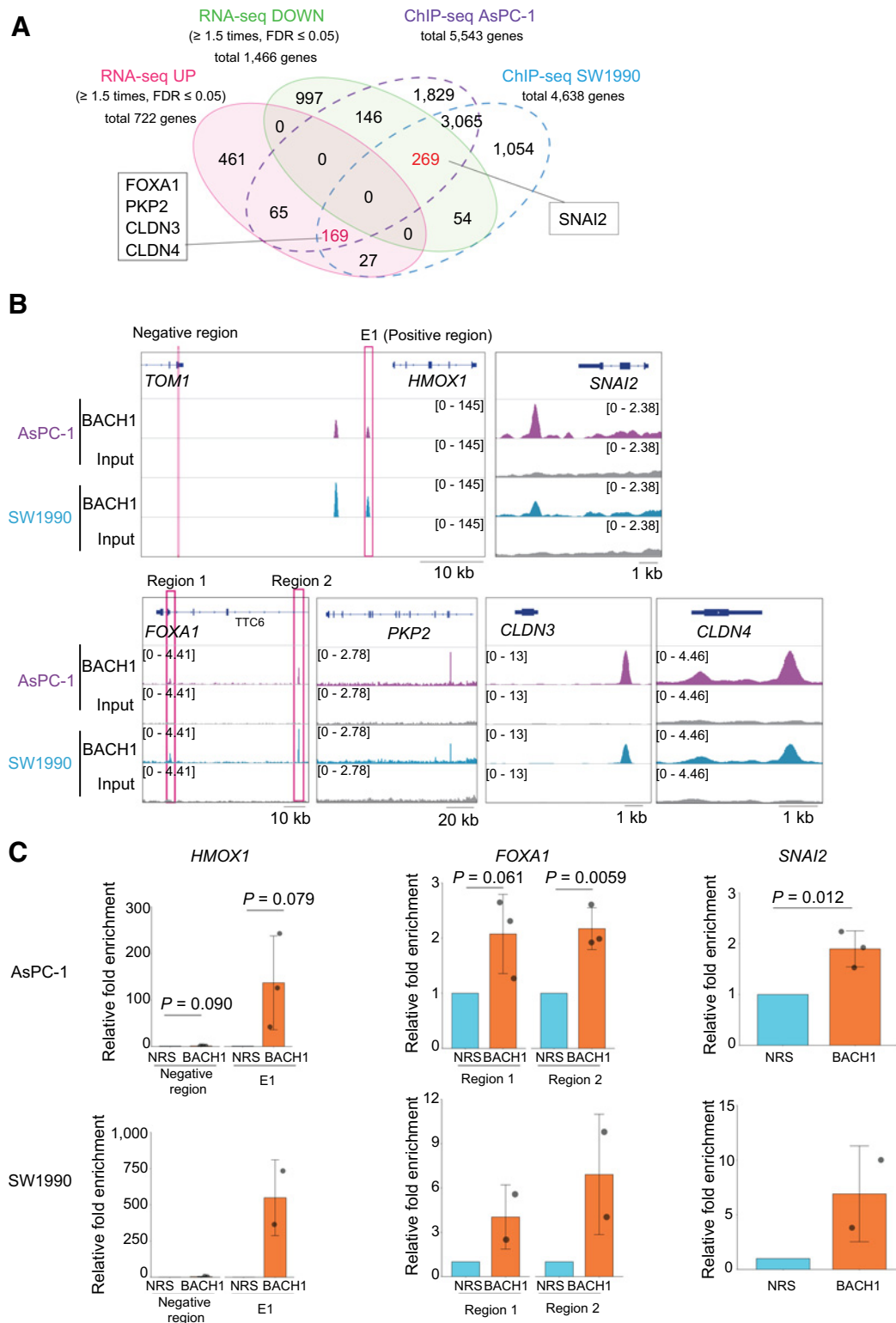
BACH1 was clearly present in the nuclei of the control pancreatic cancer cells. E-cadherin was more homogeneously stained in cell clusters of AsPC-1/*sgBACH1-2* than in those of control cells in the pancreas. A clearer accumulation of E-cadherin in the cell-cell contact region was apparent in *BACH1*-deficient cells compared with the

control cells. The metastatic cells in the liver showed similar expression patterns of E-cadherin between AsPC-1/*sgCont* and AsPC-1/*sgBACH1-2*. These results indicate that BACH1 is not required for tumor proliferation in the pancreas, but is required for efficient metastases *in vivo*.

**Figure 4.**

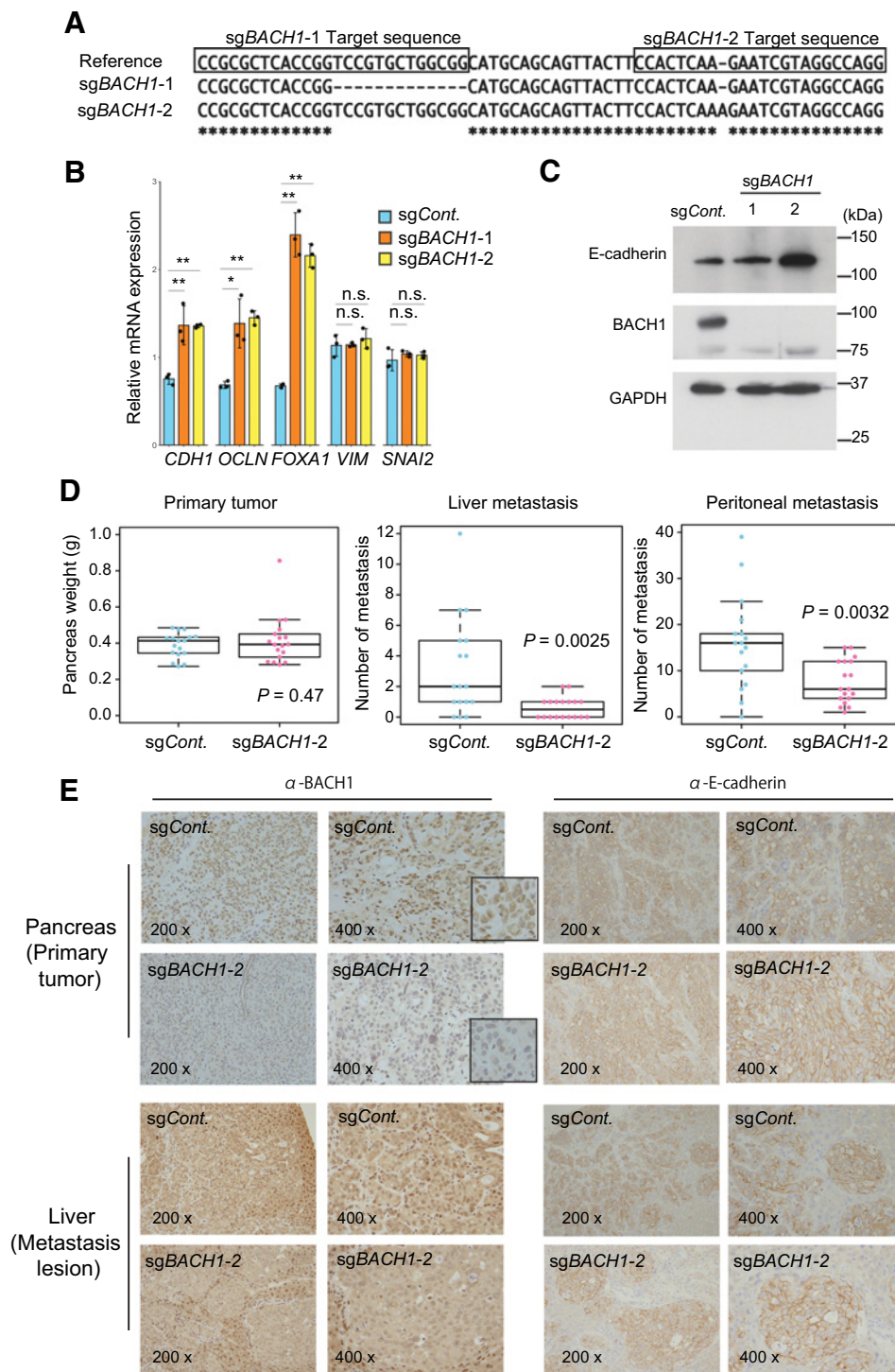
BACH1 promotes cell migration and invasion. **A**, Wound-healing assay of *BACH1*-silenced AsPC-1 cells. Scrambled siRNA was used as control. Representative photos (left) and area of wound closure (right) are shown. Scale bar, 100 μ m. **B**, Wound-healing assay of BACH1-overexpressing Panc-1 cells. Empty vector (EV) was used as control. Representative photos and area of wound closure are shown. Scale bar, 1,000 μ m. **C**, Transwell assay of *BACH1*-silencing AsPC-1 and SW1990 cells. Scrambled siRNA was used as control. Representative photos and numbers of migration or invasion cells are shown. Scale bar, 100 μ m. All data are presented as mean \pm SD, with *P* values from the Student *t* test. *, *P* < 0.05; **, *P* < 0.01.

Addition of Pancreatic Cancer to BACH1 in EMT

**Figure 5.**

BACH1 directly controls a set of EMT-related genes. **A**, Venn diagram of genes showing ≥ 1.5 -fold up (RNA-seq UP) and down (RNA-seq DOWN) regulation in BACH1 knockdown samples compared with control samples from RNA-seq (**Fig. 2**) and putative target genes of BACH1, which were detected in ChIP-seq analysis on AsPC-1 and SW1990. **B**, ChIP-seq binding profiles for the BACH1 in AsPC-1 and SW1990. **C**, ChIP-qPCR analysis of *HMOX1*, *FOXA1*, and *SNAI2* in AsPC-1 and SW1990 cells. Relative fold change is normalized to Normal Rabbit Serum (NRS). All data are presented as mean \pm SD, with *P* values from the Student *t* test.

Sato et al.

**Figure 6.**

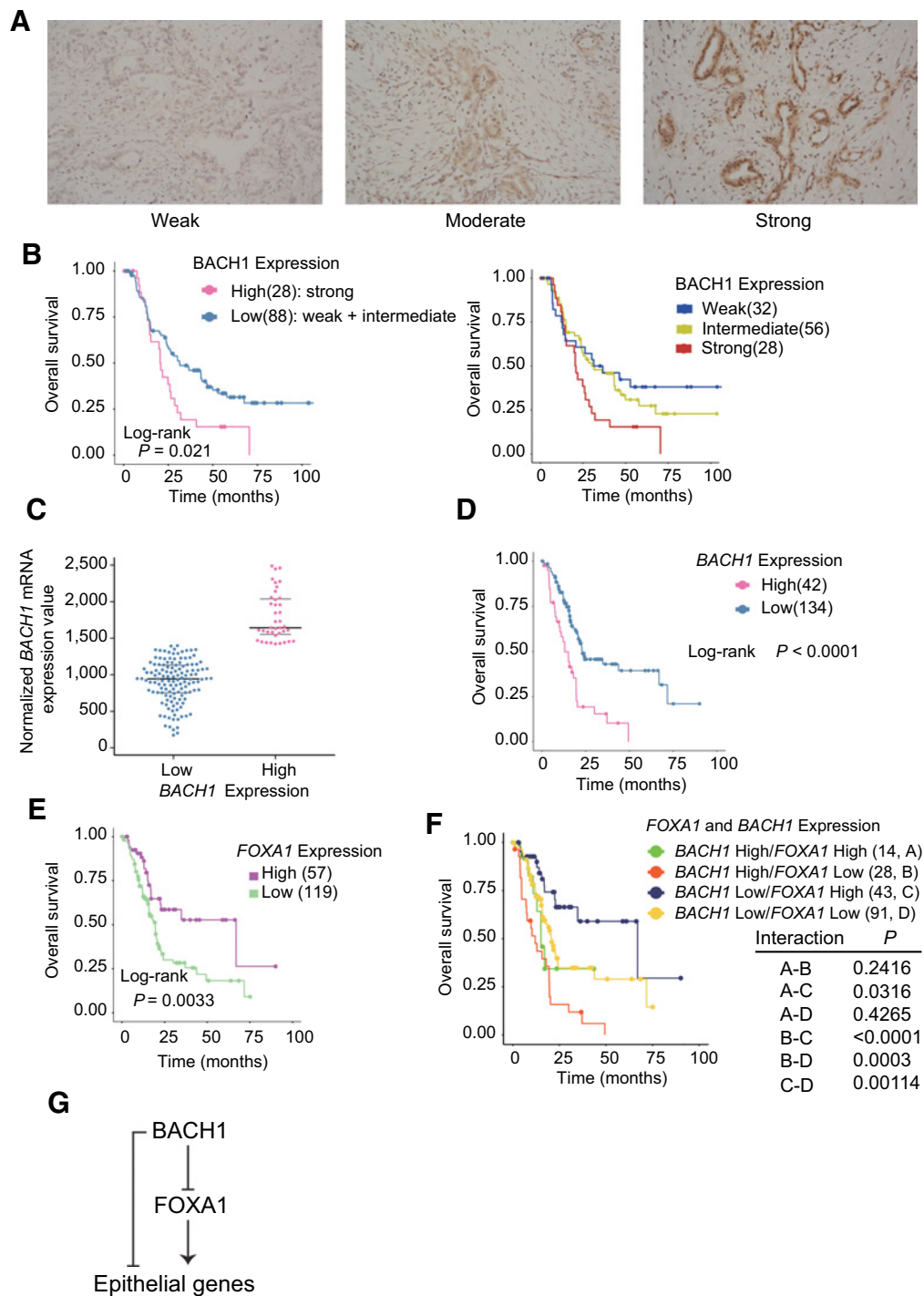
BACH1 promotes metastasis but not tumor formation. **A**, The sequences of two sgRNAs for *BACH1* and its corresponding insertion and deletion sites in the human genome. * and - indicate the presence of the same base in all sequences and the gap, respectively. **B**, Relative expression levels of the indicated transcripts of genes by qRT-PCR (relative to *ACTB* as a control). All data are presented as mean \pm SD, with *P* values from the Student *t* test. *, *P* < 0.05; **, *P* < 0.01; n.s., not significant. **C**, Immunoblot analysis of BACH1 and E-cadherin in BACH1 WT and KO AsPC-1 cells. **D**, Pancreas weight and number of liver and peritoneal metastasis (WT, *n* = 17; KO, *n* = 18). The lower end of the box shows 25% of the data, the upper end shows 75%, the middle line shows the median value, and the beard shows the maximum value or minimum value. *P* values are from the Student *t* test. **E**, Immunocytochemistry analysis of BACH1 and E-cadherin in the primary tumor and liver metastasis lesion. Magnification, $\times 200$ or $\times 400$.

High expression of BACH1 is correlated with poor prognosis

IHC analysis of clinical specimens was performed to investigate if BACH1 expression is correlated with clinicopathologic factors and prognosis. For this purpose, we generated mAb against human BACH1. On the basis of the intensity of staining, patients were classified into three groups (weak, moderate, and strong; Fig. 7A). For the following analysis, these three groups were collapsed into two groups: strong staining intensity was used as the BACH1-high expres-

sion group, whereas the groups of weak and moderate staining intensities were combined to form the BACH1-low expression group. There was no significant difference in clinicopathologic factors between these two groups (Supplementary Table S4). However, overall survival (OS) rate was significantly lower in the BACH1-high expression group (Fig. 7B left). Similar results were obtained using three groups (weak, moderate, and strong; Fig. 7B right). In univariate analysis, lymph node metastasis, distant metastasis, and BACH1-high

Addition of Pancreatic Cancer to BACH1 in EMT

**Figure 7.**

BACH1-high expression is correlated with poor prognosis. **A**, BACH1 IHC of PDAC specimens was performed and classified into three groups according to staining ratio (weak, moderate, and strong). Weak and moderate were classified as BACH1-low group, and strong was classified as BACH1-high group. Magnification, $\times 200$. **B**, Overall survival curve by Kaplan-Meier method between the two groups (high and low) based on BACH1 expression levels (left) or the three groups (strong, moderate, and weak; right). P value was obtained by log-rank test. **C**, RNA-sequencing data obtained from the TCGA ($n = 176$) were classified into two groups (BACH1 Low and High), with cut-off values obtained from the ROC curve. **D**, Overall survival curve by the Kaplan-Meier method between the two groups in **C** is shown. P value was obtained by log-rank test. **E**, RNA-sequencing data obtained from the TCGA ($n = 176$) were classified into two groups (FOXA1 Low and High), with cut-off values obtained from the ROC curve. Overall survival curve by the Kaplan-Meier method between the two groups is shown. P value was obtained by log-rank test. **F**, Overall survival curve by the Kaplan-Meier method between the four groups (combination of BACH1 and FOXA1) is shown. P value was obtained by log-rank test. **G**, A model of GRN for epithelial gene regulation. This structure suggests that steady state of the network is sensitive to signals that regulate BACH1.

Sato et al.

expression were detected as prognostic factors for OS. Multivariate analysis with the Cox proportional hazard model (28) revealed that lymph node metastasis and BACH1 high expression were the independent prognostic factors for OS (Supplementary Table S5). These results indicate that high expression of BACH1 is correlated with poor prognosis in PDAC.

When it is necessary to rely on mRNA expression, activity of transcription factors such as BACH1 may be more accurately assessed by combining expression levels of both the transcription factor and those of downstream target genes as an indication of the activity of the total transcriptional network. To test this idea, RNA-sequencing and clinical data were obtained from the TCGA database. The data were separated into two groups based on BACH1 mRNA expression levels; BACH1 low and high (Fig. 7C). OS rate of the BACH1-high expression group was significantly lower than that of the BACH1-low expression group (Fig. 7D), but there was no significant difference in clinicopathologic factors (Supplementary Table S6). In contrast, the expression of FOXA1 was positively correlated with OS rate (Fig. 7E). When FOXA1 and BACH1 were combined (Fig. 7F), the OS rate was the lowest in the group with BACH1-high expression and FOXA1-low expression, whereas it was the highest in the group with low BACH1 and high FOXA1 expression. Thus, this type of combinational analysis has improved patient stratification when compared with the usage of mRNA levels of BACH1 or FOXA1 mRNA levels alone. Other combinations of genes showed similar improvements (Supplementary Fig. S7). For example, the BACH1 high and CDH1 low group showed poorer survival than the BACH1-low and CDH1-high group. However, low expression of both BACH1 and CDH1 showed the highest OS. Furthermore, when used on its own, high CDH1 expression showed poorer survival than the CDH1 low group. Therefore, BACH1 expression may provide a useful marker for stratification of patients with PDAC.

Discussion

EMT is one of the mechanisms by which cancer cells acquire metastatic potential through loss of adherence to surrounding cells and by enhancing mobility and invasiveness (29–32). EMT is characterized by decreased quantities of epithelial adhesion molecules such as E-cadherin and increased amounts of mesenchymal molecules typified by vimentin (33). We showed here that BACH1 represses the expression of a set of epithelial genes to maintain EMT and to promote metastasis in PDAC.

We found that genes important for the regulation or structure of epithelia such as FOXA1, PKP2, CLDN3, and CLDN4 were directly repressed by BACH1, whereas EMT-promoting transcription factor SNAI2 was directly activated by BACH1 in PDAC. The results of comparison of siRNA and knockout experiments in AsPC-1 cells and overall survival analysis suggest that FOXA1 may be one of the important targets of BACH1 in PDAC. In addition to these genes, CDH1 appears indirectly but tightly regulated by BACH1. We suggest that the observed suppression of the epithelial phenotype and repression of CDH1 by BACH1 can be explained by the structure of the gene regulatory network (GRN) discovered in this study. BACH1 inhibits the expression of CDH1 by repressing FOXA1 and activating SNAI2, the activator and repressor genes of CDH1, respectively (18, 24). This study also suggests the presence of additional transcription factor(s) for activating CDH1 upon reduction of BACH1 function. When epithelial genes are aggregated, BACH1 is suggested to form a GRN involving a coherent type 2 feed-forward loop (34) in PDAC cells (Fig. 7G). Such a circuit structure is expected to confer not only

efficient suppression of the epithelial phenotype, but also rapid reexpression of this epithelial phenotype by transcription factors including FOXA1 once BACH1 is inactivated. However, the response of BACH1-overexpressing Panc-1 cells to BACH1 knockdown suggests that this GRN may fail to regulate epithelial genes in a dynamic manner under some circumstances. Our findings are consistent with epigenetic regulation by BACH1 (10) and warrant further studies on reversibility and irreversibility of BACH1-mediated regulation.

The reduction of SNAI2 expression in response to both knockdown and overexpression of BACH1 points to the importance of a proper regulation of the expression and function of SNAI2. SNAI2 expression is also regulated by XBP-1, a regulator of endoplasmic stress response, and KLF10, an effector of TGF β signaling pathway, in cancer cells (35, 36). The promotion of motility and scattering of pancreatic cancer cells by SNAI2 overexpression are observed only when Rho-associated protein kinase ROCK1/2 is inhibited (37). Therefore, the final output of BACH1 on SNAI2 and EMT may be modulated by its protein amount and other factors converging upon SNAI2.

Recently, Pastushenko and colleagues showed the presence of subspecies of PDAC cells, each representing a transition stage of EMT, based on cell surface markers (38). Among them, the cells exhibiting high metastatic potential are not the most advanced stage of EMT but an earlier stage (38). This highly metastatic stage may be configured by BACH1, which represses the expression of epithelial genes and activates only SNAI2 among mesenchymal genes. Another important possibility emerging from this study is that BACH1 is relevant to the dynamic nature of EMT and MET upon metastasis. There are two important steps in forming metastatic lesions of cancer cells. One is the migration of cancer cells caused by EMT and the other is the initiation of colonization and growth by MET at the metastatic lesions (39). We surmise that heme may be one of triggers of MET because BACH1 is exported out of the nucleus and inactivated by heme (40). The liver is one of the organs with very active heme biosynthesis in the body. When incipient metastatic cancer cells with BACH1-high expression reach the liver, heme may inactivate the BACH1 protein, causing MET. Consistent with this idea, there was no apparent difference in the expression of E-cadherin between the metastatic control and BACH1-deficient AsPC-1 cells in the liver.

Metastasis and recurrence aggravate cancer prognosis (41). Our results suggest that a higher expression of BACH1 causes poor prognosis of PDAC. While BACH1 can be inactivated by nuclear exclusion (42) or phosphorylation (43), we showed that this issue can be circumvented by analyzing both expression of BACH1 and its target genes like FOXA1. Prediction of prognosis and other phenotypes of cancer can be improved by knowledge of key GRNs. Recently, Roe and colleagues showed that, while FOXA1 acts as an antagonist of EMT, it can induce enhancer remodeling to promote metastasis of a certain subtype of PDAC (44). Therefore, a combination of BACH1 and downstream target genes can be an excellent prognostic biomarker of PDAC (Fig. 7F).

During the course of revision of this article, it has been reported that lung cancer metastasis is promoted by BACH1 in a RAS-driven mouse model (45, 46). Our results suggest that diverse epithelial cancers may utilize BACH1 to alter transiently their EMT phenotype. This is consistent with a recent finding that, while loss of E-cadherin increases invasion, it is required for systemic dissemination and seeding phases of metastasis (47). One article also reports that SNP in the 3' untranslated region of human BACH1 mRNA is associated with pancreatic cancer, suggesting BACH1 as a tumor suppressor (48). Because BACH1 is required for a proper mitosis (41), it may also play a tumor suppressor function in some stages of cancer formation, possibly in earlier stages. It

will be important to unveil how the function of BACH1 is regulated dynamically from incipient to metastatic processes of cancer.

Disclosure of Potential Conflicts of Interest

No potential conflicts of interest were disclosed.

Authors' Contributions

Conception and design: M. Sato, M. Matsumoto, K. Igarashi
Development of methodology: M. Sato, M. Matsumoto, H. Nishizawa
Acquisition of data (provided animals, acquired and managed patients, provided facilities, etc.): M. Sato, M. Matsumoto, Y. Saiki, M. Alam, H. Nishizawa, M. Rokugo, A. Brydun, M.K. Kaneko, R. Funayama, M. Ito, K. Nakayama, M. Unno
Analysis and interpretation of data (e.g., statistical analysis, biostatistics, computational analysis): M. Sato, M. Matsumoto, Y. Saiki, K. Igarashi
Writing, review, and/or revision of the manuscript: M. Sato, M. Matsumoto, M. Unno, K. Igarashi
Administrative, technical, or material support (i.e., reporting or organizing data, constructing databases): M. Matsumoto, Y. Saiki, S. Yamada, Y. Kato, M. Unno
Study supervision: M. Matsumoto, M. Unno, K. Igarashi

References

- Mann KM, Ying H, Juan J, Jenkins NA, Copeland NG. KRAS-related proteins in pancreatic cancer. *Pharmacol Ther* 2016;168:29–42.
- Garcia-Santos EP, Padilla-Valverde D, Villarejo-Campos P, Murillo-Lazaro C, Fernandez-Grande E, Palomino-Munoz T, et al. The utility of hyperthermic intra-abdominal chemotherapy with gemcitabine for the inhibition of tumor progression in an experimental model of pancreatic peritoneal carcinomatosis, in relation to their behavior with pancreatic cancer stem cells CD133+ CXCR4. *Pancreatology* 2016;16:632–9.
- Bailey P, Chang DK, Nones K, Johns AL, Patch AM, Gingras MC, et al. Genomic analyses identify molecular subtypes of pancreatic cancer. *Nature* 2016;531:47–52.
- Yachida S, Jones S, Bozic I, Antal T, Leary R, Fu B, et al. Distant metastasis occurs late during the genetic evolution of pancreatic cancer. *Nature* 2010;467:1114–7.
- Makohon-Moore AP, Zhang M, Reiter JG, Bozic I, Allen B, Kundu D, et al. Limited heterogeneity of known driver gene mutations among the metastases of individual patients with pancreatic cancer. *Nat Genet* 2017;49:358–66.
- Fitzgerald TL, Lertpiriyapong K, Cocco L, Martelli AM, Libra M, Candido S, et al. Roles of EGFR and KRAS and their downstream signaling pathways in pancreatic cancer and pancreatic cancer stem cells. *Adv Biol Regul* 2015;59:65–81.
- Igarashi K, Kurosaki T, Roychoudhuri R. BACH transcription factors in innate and adaptive immunity. *Nat Rev Immunol* 2017;17:437–50.
- Dohi Y, Ikura T, Hoshikawa Y, Katoh Y, Ota K, Nakanome A, et al. Bach1 inhibits oxidative stress-induced cellular senescence by impeding p53 function on chromatin. *Nat Struct Mol Biol* 2008;15:1246–54.
- Ota K, Dohi Y, Brydun A, Nakanome A, Ito S, Igarashi K. Identification of senescence-associated genes and their networks under oxidative stress by the analysis of Bach1. *Antioxid Redox Signal* 2011;14:2441–51.
- Fang M, Hutchinson L, Deng A, Green MR. Common BRAF(V600E)-directed pathway mediates widespread epigenetic silencing in colorectal cancer and melanoma. *Proc Natl Acad Sci U S A* 2016;113:1250–5.
- Liang Y, Wu H, Lei R, Chong RA, Wei Y, Lu X, et al. Transcriptional network analysis identifies BACH1 as a master regulator of breast cancer bone metastasis. *J Biol Chem* 2012;287:33533–44.
- Lee J, Yesilkamal AE, Wynne JP, Frankenberger C, Liu J, Yan J, et al. Effective breast cancer combination therapy targeting BACH1 and mitochondrial metabolism. *Nature* 2019;568:254–8.
- Nakanome A, Brydun A, Matsumoto M, Ota K, Funayama R, Nakayama K, et al. Bach1 is critical for the transformation of mouse embryonic fibroblasts by Ras (V12) and maintains ERK signaling. *Oncogene* 2013;32:3231–45.
- Matsumoto M, Kondo K, Shiraki T, Brydun A, Funayama R, Nakayama K, et al. Genomewide approaches for BACH1 target genes in mouse embryonic fibroblasts showed BACH1-Pparg pathway in adipogenesis. *Genes Cells* 2016;21:553–67.
- Maruyama A, Tsukamoto S, Nishikawa K, Yoshida A, Harada N, Motojima K, et al. Nrf2 regulates the alternative first exons of CD36 in macrophages through specific antioxidant response elements. *Arch Biochem Biophys* 2008;477:139–45.
- Javaid S, Zhang J, Smolen GA, Yu M, Wittner BS, Singh A, et al. MAPK7 regulates EMT features and modulates the generation of CTCs. *Mol Cancer Res* 2015;13:934–43.
- Shang X, Lin X, Alvarez E, Manorek G, Howell SB. Tight junction proteins Claudin-3 and Claudin-4 control tumor growth and metastases. *Neoplasia* 2012;14:974–IN22.
- Song Y, Washington MK, Crawford HC. Loss of FOXA1/2 is essential for the epithelial-to-mesenchymal transition in pancreatic cancer. *Cancer Res* 2010;70:2115–25.
- Xu Y, Qin L, Sun T, Wu H, He T, Yang Z, et al. Twist1 promotes breast cancer invasion and metastasis by silencing Foxa1 expression. *Oncogene* 2017;36:1157–66.
- Kumar K, Chow CR, Ebine K, Arslan AD, Kwok B, Bentrem DJ, et al. Differential regulation of ZEB1 and EMT by MAPK-interacting protein kinases (MNK) and eIF4E in pancreatic cancer. *Mol Cancer Res* 2016;14:216–27.
- Sheng W, Chen C, Dong M, Wang G, Zhou J, Song H, et al. Calreticulin promotes EGF-induced EMT in pancreatic cancer cells via Integrin/EGFR-ERK/MAPK signaling pathway. *Cell Death Dis* 2017;8:e3147.
- David CJ, Huang YH, Chen M, Su J, Zou Y, Bardeesy N, et al. TGF-beta tumor suppression through a lethal EMT. *Cell* 2016;164:1015–30.
- Witte D, Otterbein H, Forster M, Giehrl K, Zeiser R, Lehnert H, et al. Negative regulation of TGF-beta1-induced MKK6-p38 and MEK-ERK signalling and epithelial-mesenchymal transition by Rac1b. *Sci Rep* 2017;7:17313.
- Carpenter RL, Paw I, Dewhirst MW, Lo HW. Akt phosphorylates and activates HSF-1 independent of heat shock, leading to Slug overexpression and epithelial-mesenchymal transition (EMT) of HER2-overexpressing breast cancer cells. *Oncogene* 2015;34:546–57.
- Lin X, Shang X, Manorek G, Howell SB. Regulation of the epithelial-mesenchymal transition by Claudin-3 and Claudin-4. *PLoS One* 2013;8:e67496.
- Rokavec M, Kaller M, Horst D, Hermeking H. Pan-cancer EMT-signature identifies RBM47 down-regulation during colorectal cancer progression. *Sci Rep* 2017;7:4687.
- Rickelt S. Plakophilin-2: a cell-cell adhesion plaque molecule of selective and fundamental importance in cardiac functions and tumor cell growth. *Cell Tissue Res* 2012;348:281–94.
- Cox DR. Regression models and life-tables. *J R Stat Soc Series B* 1972;34:187–220.
- Peinado H, Olmeda D, Cano A. Snail, Zeb and bHLH factors in tumor progression: an alliance against the epithelial phenotype? *Nat Rev Cancer* 2007;7:415–28.
- Pickup M, Novitskiy S, Moses HL. The roles of TGFbeta in the tumour microenvironment. *Nat Rev Cancer* 2013;13:788–99.
- Joose SA, Gorges TM, Pantel K. Biology, detection, and clinical implications of circulating tumor cells. *EMBO Mol Med* 2015;7:1–11.

Acknowledgments

M. Matsumoto received Grants-in-Aid 19K07680, 16K07108, and 22700869 from the Japan Society for the Promotion of Science. Y. Kato received a grant JP18am0101078 from Agency for Medical Research and Development, Japan. K. Igarashi received Grants-in-Aid 15H02506, 24390066, 23659168, and 18H04021 from the Japan Society for the Promotion of Science. We are grateful for stimulating discussions with members of Department of Biochemistry and Department of Surgery, and Jelle Bonthuis for comments on the manuscript. We also acknowledge the technical support of the Biomedical Research Core of Tohoku University Graduate School of Medicine.

The costs of publication of this article were defrayed in part by the payment of page charges. This article must therefore be hereby marked *advertisement* in accordance with 18 U.S.C. Section 1734 solely to indicate this fact.

Received December 31, 2018; revised July 12, 2019; accepted January 6, 2020; published first January 9, 2020.

Sato et al.

32. Tsai JH, Donaher JL, Murphy DA, Chau S, Yang J. Spatiotemporal regulation of epithelial-mesenchymal transition is essential for squamous cell carcinoma metastasis. *Cancer Cell* 2012;22:725–36.
33. Vincent T, Neve EP, Johnson JR, Kukalev A, Rojo F, Albanell J, et al. A SNAIL1-SMAD3/4 transcriptional repressor complex promotes TGF-beta mediated epithelial-mesenchymal transition. *Nat Cell Biol* 2009;11:943–50.
34. Mangan S, Alon U. Structure and function of the feed-forward loop network motif. *Proc Natl Acad Sci U S A* 2003;100:11980–5.
35. Mishra VK, Subramaniam M, Kari V, Pitel KS, Baumgart SJ, Naylor RM, et al. Kruppel-like transcription Factor KLF10 suppresses TGFbeta-induced epithelial-to-mesenchymal transition via a negative feedback mechanism. *Cancer Res* 2017;77:2387–400.
36. Cuevas EP, Eraso P, Mazon MJ, Santos V, Moreno-Bueno G, Cano A, et al. LOXL2 drives epithelial-mesenchymal transition via activation of IRE1-XBP1 signalling pathway. *Sci Rep* 2017;7:44988.
37. Shields MA, Krantz SB, Bentrem DJ, Dangi-Garimella S, Munshi HG. Interplay between beta1-integrin and Rho signaling regulates differential scattering and motility of pancreatic cancer cells by snail and slug proteins. *J Biol Chem* 2012;287:6218–29.
38. Pastushenko I, Brisebarre A, Sifrim A, Fioramonti M, Revenco T, Boumahdi S, et al. Identification of the tumor transition states occurring during EMT. *Nature* 2018;556:463–8.
39. Korpai M, Ell BJ, Buffa FM, Ibrahim T, Blanco MA, Celia-Terrassa T, et al. Direct targeting of Sec23a by miR-200s influences cancer cell secretome and promotes metastatic colonization. *Nat Med* 2011;17:1101–8.
40. Sun J, Brand M, Zenke Y, Tashiro S, Groudine M, Igarashi K. Heme regulates the dynamic exchange of Bach1 and NF-E2-related factors in the Maf transcription factor network. *Proc Natl Acad Sci U S A* 2004;101:1461–6.
41. Sahin IH, Elias H, Chou JF, Capanu M, O'Reilly EM. Pancreatic adenocarcinoma: insights into patterns of recurrence and disease behavior. *BMC Cancer* 2018;18:769.
42. Suzuki H, Tashiro S, Sun J, Doi H, Satomi S, Igarashi K. Cadmium induces nuclear export of Bach1, a transcriptional repressor of heme oxygenase-1 gene. *J Biol Chem* 2003;278:49246–53.
43. Li J, Shima H, Nishizawa H, Ikeda M, Brydun A, Matsumoto M, et al. Phosphorylation of BACH1 switches its function from transcription factor to mitotic chromosome regulator and promotes its interaction with HMMR. *Biochem J* 2018;475:981–1002.
44. Roe JS, Hwang CI, Somerville TDD, Milazzo JP, Lee EJ, Da Silva B, et al. Enhancer reprogramming promotes pancreatic cancer metastasis. *Cell* 2017;170:875–88 e20.
45. Lignitto L, LeBoeuf SE, Homer H, Jiang S, Askenazi M, Karakousi TR, et al. Nrf2 activation promotes lung cancer metastasis by inhibiting the degradation of bach1. *Cell* 2019;178:316–329.
46. Wiel C, Le Gal K, Ibrahim MX, Jahangir CA, Kashif M, Yao H, et al. BACH1 stabilization by antioxidants stimulates lung cancer metastasis. *Cell* 2019;178:330–345.
47. Padmanaban V, Krol I, Suhail Y, Szczerba BM, Aceto N, Bader JS, et al. E-cadherin is required for metastasis in multiple models of breast cancer. *Nature* 2019;573:439–44.
48. Huang X, Zheng J, Li J, Che X, Tan W, Tan W, et al. Functional role of BTB and CNC homology 1 gene in pancreatic cancer and its association with survival in patients treated with gemcitabine. *Theranostics* 2018;8:3366–79.

Cancer Research

The Journal of Cancer Research (1916–1930) | The American Journal of Cancer (1931–1940)

BACH1 Promotes Pancreatic Cancer Metastasis by Repressing Epithelial Genes and Enhancing Epithelial–Mesenchymal Transition

Masaki Sato, Mitsuyo Matsumoto, Yuriko Saiki, et al.

Cancer Res 2020;80:1279-1292. Published OnlineFirst January 9, 2020.

Updated version Access the most recent version of this article at:
doi:[10.1158/0008-5472.CAN-18-4099](https://doi.org/10.1158/0008-5472.CAN-18-4099)

Supplementary Material Access the most recent supplemental material at:
<http://cancerres.aacrjournals.org/content/suppl/2020/01/08/0008-5472.CAN-18-4099.DC1>

Cited articles This article cites 48 articles, 12 of which you can access for free at:
<http://cancerres.aacrjournals.org/content/80/6/1279.full#ref-list-1>

E-mail alerts [Sign up to receive free email-alerts](#) related to this article or journal.

Reprints and Subscriptions To order reprints of this article or to subscribe to the journal, contact the AACR Publications Department at pubs@aacr.org.

Permissions To request permission to re-use all or part of this article, use this link
<http://cancerres.aacrjournals.org/content/80/6/1279>.
Click on "Request Permissions" which will take you to the Copyright Clearance Center's (CCC) Rightslink site.